CrystEngComm

Cite this: *CrystEngComm*, 2012, **14**, 401

www.rsc.org/crystengcomm

COMMUNICATION

Synthesis of Cu_3SnS_4 nanocrystals and nanosheets by using $Cu_{31}S_{16}$ as seeds†

Luoxin Yi,[ab] Dan Wang*[b] and Mingyuan Gao*[a]

Received 6th September 2011, Accepted 15th November 2011
DOI: 10.1039/c1ce06153d

Orthorhombic Cu_3SnS_4 nano-cuboids and nanosheets were synthesized by using monoclinic $Cu_{31}S_{16}$ nanocrystals as seeds. Transmission electron microscopy and powder X-ray diffractometry were adopted to investigate the resultant nanocrystals and the structural transformation of monoclinic $Cu_{31}S_{16}$ to orthorhombic Cu_3SnS_4.

Multinary semiconductor materials have attracted increasing attention due to their potential applications in photovoltaic devices,[1] nonlinear optical materials,[2] superconducting materials,[3] fluorescent materials,[4] *etc.* The physical properties of multinary semiconductors are highly abundant because the electronic structures of multinary semiconductors can largely be tuned by the stoichiometric ratio of the constituent elements. Although the physical properties as well as the preparation of thin films of various types of multinary semiconductor materials have largely been investigated, the synthesis of multinary semiconductor nanomaterials remains a hot topic. Nanometre sized semiconductors on the one hand present unique physical properties due to the quantum confinement effect. On the other hand, low cost processing techniques can facilely be used for integrating semiconductor nanoparticles into optoelectronic devices.[5–11]

Djurleite ($Cu_{31}S_{16}$) as a metal chalcogenide compound semiconductor possesses a cationic deficiency structure. At temperatures above 125 °C, $Cu_{31}S_{16}$ has only 85% of its copper sites in the hexagonally packed framework of sulfur atoms occupied,[12] which makes Cu atoms in $Cu_{31}S_{16}$ behave virtually like "fluid" supported by the fact that djurleite has large ionic conductivity above 100 °C.[13] Therefore, djurleite is an ideal host for forming multinary semiconductors with unique physical properties. For example, copper sulfide-based multinary semiconductors such as $Cu(In,Ga)(Se,S)_2$ and Cu_2ZnSnS_4 have been demonstrated to be useful in solar cells and non-linear optical materials.[14–17] Nanometre sized Cu_2ZnSnS_4 was also reported to be possibly useful in achieving low cost photovoltaics.[18–21] Nevertheless, the $Cu_{31}S_{16}$ nano-seeds do not always lead to a homogeneous structure. Our previous studies have demonstrated that by successively pyrolyzing Cu(II) acetylacetonate ($Cu(acac)_2$) and In(III) acetylacetonate ($In(acac)_3$) in dodecanethiol, Cu_2S–In_2S_3 heterostructured nanocrystals can be obtained.[22] By a similar approach, $Cu_{1.94}S$–ZnS heterostructured nanorods instead of ternary semiconductor nanocrystals are also obtained.[23] In difference, very recently we have further demonstrated that pyrolyzing $Cu(acac)_2$ in dodecanethiol in the presence of $SnCl_4$ leads to Sn doped $Cu_{31}S_{16}$ nanosheets.[24]

Following on from our previous investigations on copper sulfide-based semiconductor nanocrystals, herein we report our recent results on quasi-cuboid Cu_3SnS_4 nanocrystals and thin Cu_3SnS_4 nanosheets prepared by using faceted $Cu_{1.94}S$ nanocrystals and ultrathin $Cu_{1.94}S$ nanosheets as templates. The structural transformation of monoclinic $Cu_{31}S_{16}$ to orthorhombic Cu_3SnS_4 was also investigated.

Two synthetic routes as shown in Scheme 1 were adopted in the current investigation. In the first synthetic route, 1.00 mmol of $Cu(acac)_2$ was firstly pyrolyzed at 200 °C in 30 mL of dodecanethiol for 1 h to obtain $Cu_{31}S_{16}$ nano-seeds, into which 10 mL of dodecanethiol stock solution containing 0.50 mmol of $SnCl_4 \cdot 5H_2O$ was then intermittently injected by three times with an interval of 1 h. After that, the reaction was allowed to proceed for 4 more hours under reflux. Aliquots were extracted every hour during the preparation for monitoring the particle growth. The resultant nanocrystals were collected and purified by using ethanol as precipitant. Fig. 1a shows a representative transmission electron microscopy (TEM) image of the nanoparticles (sample 6) obtained 4 h after the last portion of

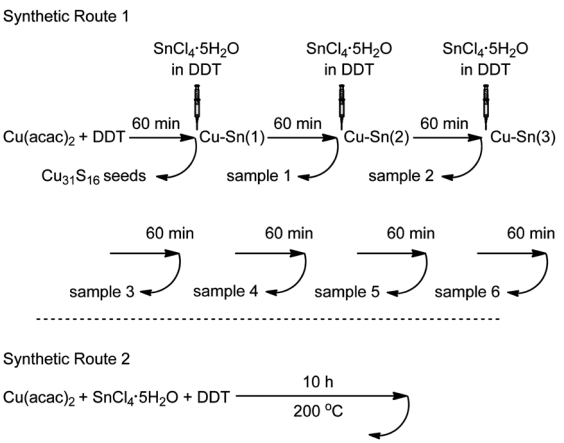

Scheme 1 Synthetic routes for Cu_3SnS_4 nanocrystals and nanosheets.

[a]*Institute of Chemistry, The Chinese Academy of Sciences, Bei Yi Jie 2, Zhong Guan Cun, Beijing, 100190, China. E-mail: gaomy@iccas.ac.cn; Fax: +86 10 82613214*
[b]*Institute of Process Engineering, The Chinese Academy of Sciences, No.1 Zhongguancun North Second Street, Beijing, 100190, China. E-mail: danwang@home.ipe.ac.cn*

† Electronic supplementary information (ESI) available: (1) Experimental details; (2) XPS analysis of sample 6; and (3) TEM, XRD, and SAED results of nanosheets obtained *via* synthetic route 2 shown in Scheme 1 by 48 min and 5 h of reflux. See DOI: 10.1039/c1ce06153d

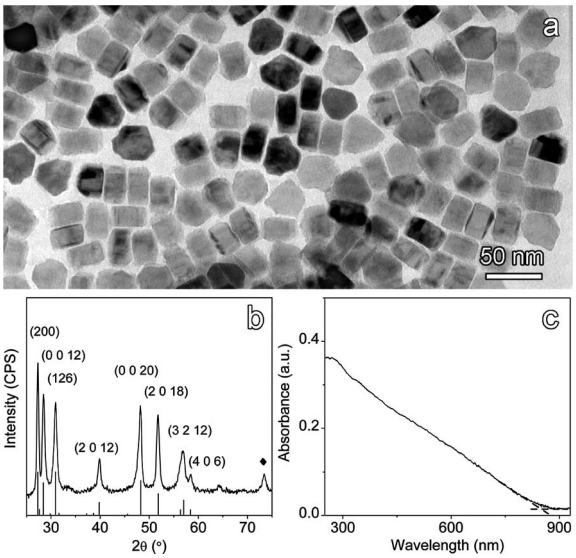

Fig. 1 TEM image (a), powder XRD pattern (b) and UV-Vis absorption spectrum (c) of sample 6. The diffraction peaks in frame (b) are labeled by the corresponding crystal planes of orthorhombic Cu_3SnS_4 whose standard diffraction data (JCPDS card 36-0217) are plotted at the bottom.

$SnCl_4$ was injected. In general, most of the resultant nanoparticles are rectangular in shape with a long-axis size of 31.8 ± 4.9 nm on average. The crystalline structure of this sample was analyzed by XRD. As shown in Fig. 1b, the major diffraction peaks can well be indexed to orthorhombic Cu_3SnS_4 (JCPDS card No. 36-0217), while the diffraction peak marked by "◆" can be assigned to the diffraction of tetragonal Cu_3SnS_4 which is often observed as a co-existing phase in orthorhombic Cu_3SnS_4 thin films prepared by the sputtering method.[25] Further XPS analysis revealed that the atomic ratio of Cu : Sn : S in this sample is around 3.54 : 1.00 : 3.81 based on Cu2p, Sn3d, and S2p core level peaks, quite close to the stoichiometric ratio within Cu_3SnS_4. More details are provided in Fig. S1 in the ESI†. The as-prepared nanocrystals can well be dispersed in tetrahydrofuran to form a colloidal solution, which allowed further characterization of their optical properties. A typical ultra-violet and visible (UV-Vis) absorption spectrum of the nanocrystals is provided in Fig. 1c. In general, the absorption spectrum is rather featureless with the absorption edge located around 840 nm (1.48 eV), slightly red-shifted in comparison with that, *i.e.*, at 800 nm (1.55 eV) for orthorhombic Cu_3SnS_4,[26] which can be understood by the existence of the trace tetragonal Cu_3SnS_4 phase. Because the absorption edge of the latter one is typically around 1016 nm (1.22 eV),[27] it is deserved to mention that no orthorhombic Cu_3SnS_4 nanoparticles have been reported before let along their optical properties. Therefore, the absorption edge herein is extracted from the cross-point of the extended lines from the absorption and non-absorption areas.

As a matter of fact, the synthesis of hexagonal Cu_2SnS_3 nanocrystals,[5] triclinic Cu_2SnS_3 nanocrystals[6,7] and tetragonal Cu_3SnS_4 nanocrystals[8,9] was previously reported. But to the best of our knowledge, the orthorhombic phase Cu_3SnS_4 nanocrystals were not reported before. Due to its suitable bandgap, orthorhombic Cu_3SnS_4 can be potentially used as an inexpensive light absorption material for solar cells. Therefore the formation of orthorhombic Cu_3SnS_4 nanocrystals was carefully followed by both TEM and XRD measurements. As shown in Fig. 2, the initial nanocrystal seeds of 17.6 ± 1.5 nm are quasi-spherical with an observable hexagonal-faceted structure. The XRD results placed aside support that seeds are monoclinic $Cu_{31}S_{16}$ nanocrystals (17.6 ± 1.5 nm). They are subsequently elongated after the first portion of $SnCl_4$ was injected and then remain nearly unchanged in shape after all three portions of $SnCl_4$ were injected. Nevertheless, the XRD patterns are gradually altered by showing new diffraction peaks at around 48.0° and 51.7° starting from sample 3 that was extracted 1 h after all $SnCl_4$ portions were introduced. These two diffraction peaks correspond to the (0 0 20) and (2 0 18) of orthorhombic Cu_3SnS_4. Upon prolonged reflux, the elongated hexagonal nanocrystals are gradually transformed into cuboid nanocrystals as shown in Fig. 2f. Along with this morphological change, the diffraction peaks of (2 0 0), (0 0 12), and (1 2 6) of orthorhombic Cu_3SnS_4 gradually develop. In the meantime, the characteristic diffraction peaks of monoclinic $Cu_{31}S_{16}$ at 37.6°, 46.3°, and 48.6° gradually vanish, accompanied by a gradual increase in the Sn/Cu ratio indicated in Fig. 2. In our previous investigations,

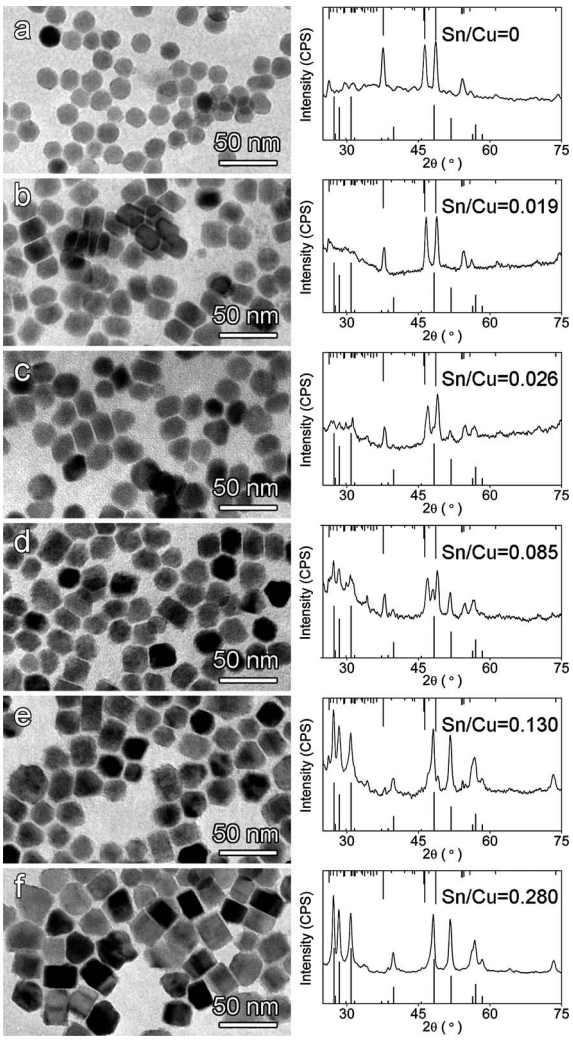

Fig. 2 TEM images of $Cu_{31}S_{16}$ nanocrystal seeds (a), sample 1 (b), sample 2 (c), sample 3 (d), sample 4 (e), and sample 5 (f) together with the corresponding XRD patterns laid aside. In each XRD frame, the standard diffraction peaks of $Cu_{31}S_{16}$ (JCPDS card 23-0959) and Cu_3SnS_4 (JCPDS card 36-0217) are placed on the top and at the bottom, respectively. In addition, the Sn/Cu ratio of each sample is also inserted.

$Cu_{31}S_{16}$ nanocrystals were used as a host matrix for indium and zinc ions, but similar preparations led to heterostructured Cu_2S–In_2S_3 and $Cu_{31}S_{16}$–ZnS nanocrystals, respectively.[19,23] In difference, the current reaction system generates ternary Cu_3SnS_4 nanocrystals rather than heterostructured ones, which suggests that Sn atoms can not only enter the copper vacancy in $Cu_{31}S_{16}$ at elevated temperature, but also change the crystal cell of $Cu_{31}S_{16}$ to give rise to the orthorhombic phase Cu_3SnS_4. Although djurleite $Cu_{31}S_{16}$ belongs to a monoclinic crystal system, the β angle is only of 90.13°, quite close to 90°. Therefore, the structural transformation of monoclinic $Cu_{31}S_{16}$ to orthorhombic Cu_3SnS_4 costs less energy than to tetragonal Cu_3SnS_4 nanocrystals which are the typical phase formed by hydrothermal synthesis.[28]

We have previously demonstrated that $SnCl_4$ has a remarkable ability in regulating the shape of $Cu_{31}S_{16}$ nanocrystals formed by pyrolyzing $Cu(acac)_2$ in dodecanethiol, because $SnCl_4$ can coordinate with dodecanethiol forming stable complexes that preferentially attach on the {100} facets of the djurleite and hinder the crystal growth along the [100] direction. Consequently ultrathin 2D Sn-doped djurleite nanocrystals can be obtained.[24] The current results shown in Fig. 1 and 2 suggest that binary $Cu_{31}S_{16}$ can be used as seeds for synthesizing ternary Cu_3SnS_4 nanocrystals. Therefore, the second synthetic route shown in Scheme 1 was adopted for synthesizing Cu_3SnS_4 nanosheets. In brief, 30 mL of dodecanethiol solution containing 1.00 mmol of $Cu(acac)_2$ and 0.50 mmol of $SnCl_4 \cdot 5H_2O$ was refluxed. During the early stage of reflux, *e.g.*, 48 min, $Cu_{31}S_{16}$ nanosheets of 209 ± 33 nm in lateral dimension and less than 1 nm in thickness were also obtained as shown in Fig. S2 in the ESI†. High-resolution TEM results provided in Fig. S3† support that the nanosheets are single crystals. However, when the reflux time reached 5 h, the nanosheets comprised of both monoclinic $Cu_{31}S_{16}$ and orthorhombic Cu_3SnS_4 phases were formed, as shown in Fig. S4 in the ESI†. Careful XRD investigations suggested that 10 h of reflux is the minimum time for achieving orthorhombic Cu_3SnS_4 as shown in Fig. 3a. The XPS elemental analysis suggests that the Cu : Sn : S ratio for the nanosheets is of 3.00 : 1.37 : 3.66, close to 3 : 1 : 4 for Cu_3SnS_4. In the meantime, the thickness of the resultant nanosheets increases to ~15 nm as indicated by the results in Fig. 3b. A representative nanosheet together with the selected area electron diffraction (SAED) pattern is shown in Fig. 3c and d, respectively. Close observation reveals that the bottom and top surfaces, *i.e.*, the original (100) facets of $Cu_{31}S_{16}$ nanosheets, are transformed into (010) facets of orthorhombic Cu_3SnS_4.

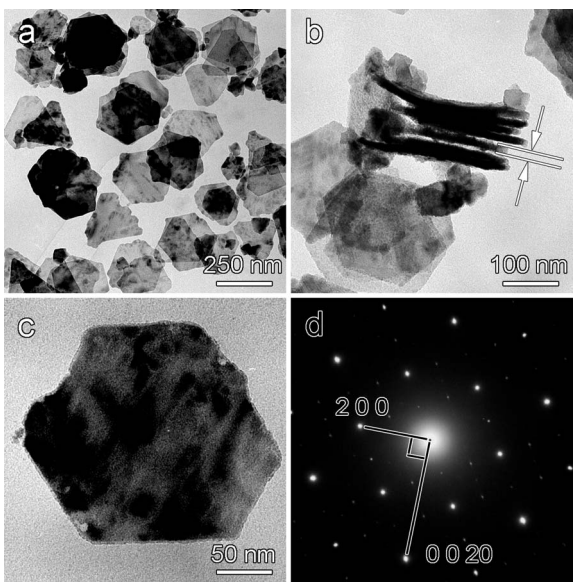

Fig. 3 TEM images of the nanosheets obtained by 10 h of reflux *via* synthetic route 2 (a–c) and the SAED pattern (d) of the single nanosheet shown in frame (c).

In summary, it has successfully been demonstrated that ternary orthorhombic Cu_3SnS_4 nanocrystals can be synthesized by using $Cu_{31}S_{16}$ as seeds owing to the cationic deficiency structure of $Cu_{31}S_{16}$ at elevated temperature. As the shapes of the $Cu_{31}S_{16}$ seeds can largely be preserved during the synthesis, quasi-cuboid Cu_3SnS_4 nanocrystals and Cu_3SnS_4 thin nanosheets are obtained by using faceted $Cu_{31}S_{16}$ nanocrystals and ultrathin $Cu_{31}S_{16}$ nanosheets as template, respectively. The current investigation therefore suggests that taking the advantage of the cationic deficiency structure of $Cu_{31}S_{16}$, different copper sulfide-based multinary semiconductor nanocrystals can potentially be obtained by using nanostructured $Cu_{31}S_{16}$ as template.

Acknowledgements

The authors thank National Basic Research Program of China (2011CB935800), MOST (2010AA06Z302), and Croucher Foundation (9220054) for financial support.

Notes and references

1 L. Li, N. Coates and D. Moses, *J. Am. Chem. Soc.*, 2010, **132**, 22.
2 H. S. Ra, K. M. Ok and P. S. Halasyamani, *J. Am. Chem. Soc.*, 2003, **125**, 7764.
3 M. Miyakawa, S. W. Kim, M. Hirano, Y. Kohama, H. Kawaji, T. Atake, H. Ikegami, K. Kono and H. Hosono, *J. Am. Chem. Soc.*, 2007, **129**, 7270.
4 T. Torimoto, T. Adachi, K. Okazaki, M. Sakuraoka, T. Shibayama, B. Ohtani, A. Kudo and S. Kuwabata, *J. Am. Chem. Soc.*, 2007, **129**, 12388.
5 C. Z. Wu, Z. P. Hu, C. L. Wang, H. Sheng, J. L. Yang and Y. Xie, *Appl. Phys. Lett.*, 2007, **91**, 143104.
6 B. Li, Y. Xie, J. X. Huang and Y. T. Qian, *J. Solid State Chem.*, 2000, **153**, 170.
7 S. Bloss and M. Jansen, *Z. Naturforsch., B: J. Chem. Sci.*, 2003, **58**, 1075.
8 X. Y. Chen, X. Wang, C. H. An, J. W. Liu and Y. T. Qian, *J. Cryst. Growth*, 2003, **256**, 368.
9 Y. J. Xiong, Y. Xie, G. A. Du and H. L. Su, *Inorg. Chem.*, 2002, **41**, 2953.
10 T. Howard and J. Evans, *Z. Kristallogr.*, 1979, **150**, 299.
11 M. Y. Gao, C. Lesser, S. Kirstein, H. Möhwald, A. L. Rogach and H. Weller, *J. Appl. Phys.*, 2000, **87**, 2297.
12 M. Y. Gao, B. Richter, S. Kirstein and H. Möhwald, *J. Phys. Chem. B*, 1998, **102**, 4096.
13 E. Hirahara, *J. Phys. Soc. Jpn.*, 1951, **6**, 428.
14 M. G. Panthani, V. Akhavan, B. Goodfellow, J. P. Schmidtke, L. Dunn, A. Dodabalapur, P. F. Barbara and B. A. Korgel, *J. Am. Chem. Soc.*, 2008, **130**, 16770.
15 D. J. Bottomley, A. Mito, S. Niki and A. Yamada, *J. Appl. Phys.*, 1997, **82**, 817.
16 A. Weber, R. Mainz, T. Unold, S. Schorr and H. W. Schock, *Phys. Status Solidi C*, 2009, **6**, 1245.
17 F. Long, W. M. Wang, H. C. Tao, T. K. Jia, X. M. Li, Z. Zou and Y. Fu, *Mater. Lett.*, 2010, **64**, 195.
18 S. C. Riha, B. A. Parkinson and A. L. Prieto, *J. Am. Chem. Soc.*, 2009, **131**, 12054.
19 Q. J. Guo, H. W. Hillhouse and R. Agrawal, *J. Am. Chem. Soc.*, 2009, **131**, 11672.

20 C. Steinhagen, M. G. Panthani, V. Akhavan, B. Goodfellow, B. Koo and B. A. Korgel, *J. Am. Chem. Soc.*, 2009, **131**, 12554.
21 X. Lu, Z. Zhuang, Q. Peng and Y. Li, *Chem. Commun.*, 2011, **47**, 3141.
22 W. Han, L. Yi, N. Zhao, A. Tang, M. Gao and Z. Tang, *J. Am. Chem. Soc.*, 2008, **130**, 13152.
23 L. X. Yi, A. W. Tang, M. Niu, W. Han, Y. B. Hou and M. Y. Gao, *CrystEngComm*, 2010, **12**, 4124.
24 L. X. Yi and M. Y. Gao, *Cryst. Growth Des.*, 2011, **11**, 1109.
25 P. A. Fernandes, P. M. P. Salome and A. F. da Cunha, *J. Phys. D: Appl. Phys.*, 2010, **43**, 215403.
26 P. A. Fernandes, P. M. P. Salome and A. F. da Cunha, *Phys. Status Solidi C*, 2010, **7**, 901.
27 M. Bouaziz, J. Ouerfelli, M. Amlouk and S. Belgacem, *Phys. Status Solidi A*, 2007, **204**, 3354.
28 H. M. Hu, Z. P. Liu, B. J. Yang, X. Y. Chen and Y. T. Qian, *J. Cryst. Growth*, 2005, **284**, 226.

